

Received February 12, 2019, accepted February 18, 2019, date of publication February 22, 2019, date of current version March 12, 2019.

Digital Object Identifier 10.1109/ACCESS.2019.2901220

# A Novel Three-Dimensional Integrated Spoof Surface Plasmon Polaritons Transmission Line

SENSONG SHEN<sup>1</sup>, BING XUE<sup>1,2</sup>, MENGXIA YU<sup>1</sup>, AND JUN XU<sup>1</sup>

<sup>1</sup>School of Physics, University of Electronic Science and Technology of China, Chengdu 610054, China

<sup>2</sup>Institute of Electronics, Chinese Academy of Sciences, Beijing 100190, China

Corresponding author: Bing Xue (xuebing14@mails.ucas.ac.cn)

This work was supported by the Millimeter-wave Circuits and Systems Laboratory, School of Physics, University of Electronic Science and Technology of China.

**ABSTRACT** In this paper, a novel three-dimensional integrated spoof surface plasmon polaritons (SSPPs) transmission line (TL) is proposed. The controlled slow surface wave can propagate along unit cells that are planted on a metal strip periodically, which is similar to the typical SSPPs TLs. The dispersion characteristics and high-order modes of the proposed TL are studied. In order to verify the transmission performance of the proposed TL, a two-dimensional (2D) structure is utilized to do like the conversion. We have designed the proposed TL and give the simulated results from 10–25GHz, which show good propagation performance. The ohmic losses and dielectric losses of the proposed TL and typical 2D SSPPs TLs are simulated and compared with the microstrip line, coplanar waveguide. The measured data for the proposed TL indicates that the measured results are close to the simulations. The low-loss and highly integrated characteristics of the proposed TL plays an important role in the microwave and terahertz SSPPs transmission and integrated circuits.

**INDEX TERMS** Spoof surface plasmon polaritons (SSPPs), dispersion characteristics, high-order modes, loss characteristics.

## I. INTRODUCTION

Surface plasmon polaritons (SPPs) are electromagnetic waves formed by light incident on a metal surface, which propagate along the interface of air-metal and decay exponentially in the transverse direction. It has extensive research in the optical field, and has broad application prospects in the fields of biomedicine, chemical sensing and micro-nano photonics [1]–[7]. Hereafter, the abnormal transmission phenomenon of freely propagating coherent terahertz radiation through free-standing metal foils perforated with periodic arrays of sub-wavelength apertures was observed experimentally by Gómez Rivas *et al.* [8], Cao and Nahata [9], [10]. Pendry *et al.* proposed a new theory for the surface plasmon polariton-like bound surface states, which is called spoof surface plasmon polaritons (SSPPs), thus unifying the similar phenomena in microwave and optical frequencies [11], [12]. The prominent advantages of SSPPs structure are that its dispersion characteristics and the ability to confine

electromagnetic waves are completely determined by its structural size. The presentation of SSPPs extends its research scope from optical field to terahertz and microwave frequencies, greatly expanding its application range. A variety of devices had been proposed and studied, such as the three-dimensional (3D) terahertz splitter and bending slow-wave system [13], 3D terahertz switch [14] and 3D terahertz polarizer controller [15].

As the foundation of microwave devices and systems, transmission lines (TLs) combine different types of devices into multiple functional systems by delivering electromagnetic power or signals. The SSPPs TLs for terahertz and microwave frequencies are 3D structures in the early days, which can propagate along periodic etched grooves or gaps in metal conductors [16], [17]. Since then, a variety of different 3D TLs have been proposed [18]–[21]. However, such TLs are difficult to process and are costly. A two-dimensional (2D) SSPPs planar TL is proposed, which is realized by a single-line strip-shaped metal with periodically arranged grooves. It not only has advantages of high field confinement and controllable dispersion properties, but also

The associate editor coordinating the review of this manuscript and approving it for publication was Kai-Da Xu.

have pliable properties and can fabricate directly by printed circuit board (PCB) process [22]. Subsequently, conversion structures of coplanar waveguide (CPW) and microstrip line to SSPPs TLs are proposed, making it possible to study and measure their transmission performance [23]–[25]. Moreover, the SSPPs structures can support high-order modes, which is similar to some traditional microwave TLs. The high-order modes of SSPPs supported by periodically corrugated metal surfaces were investigated theoretically. The expression for the existence condition of high-order modes was presented [26]. And then, the high-order mode SSPPs for terahertz sensing was been investigated [27]. More recently, the terahertz high-order mode broadband SSPPs propagation is proposed for the first time, which indicates that high-order mode transmission has significant potential for application at microwave and terahertz frequencies [28]. Meanwhile, linear and nonlinear microwave devices based on SSPPs TLs have been proposed, which lays the foundation for the future establishment of SSPP system [29]–[37].

The existed substrate integrated SSPPs TLs are 2D conversion structures that make them difficult to integrate with classical 3D TLs such as microstrip lines. Although the conversion structure from microstrip line to SSPPs TL is proposed, the conversion efficiency is low and the loss is high [24], [25]. In contrast, the 3D TL that can be integrated on the PCB has a wider range of applications. An integrated 3D TL is proposed recently, which is implemented on a single-layer substrate with metallized via holes planted on a ground plane and excited by substrate integrated waveguide (SIW) working at Ka band [38]. This TL has profound implications in the microwave frequency, its structure is semi-open and the anti-interference ability is similar to the microstrip line. However, the feeding method and performance of this TL are poor, which limits the practical application. In [38], ohmic loss, dielectric loss and radiation loss of this TL are not studied respectively. Although the total losses has been studied, it is still not accurate due to the radiation loss varies nonlinearly with the length of SSPPs TL [39]. It is more reasonable to study the ohmic loss, dielectric loss and radiation loss for these SSPPs structure separately.

This paper, based on [38], proposes a new SSPPs 3D TL, which can also be integrated with microwave circuits and has more advantageous ways of adjusting the dispersion characteristics and more flexible TL configurations. The possibility of applying SSPPs TLs to microwave integrated circuits has been greatly increased. A simple high-efficiency 2D conversion structure is utilized to convert the CPW guided waves to the proposed TL, which has a more compact structure and better performance than [38].

This paper is organized as follow. Section II gives the dispersion characteristics and field distributions of fundamental and high-order modes. Section III gives the conversion structure of the proposed TL connected to CPW and simulated scattering parameters (S-parameters). In the Section IV, the ohmic losses and dielectric losses of the proposed TL and some typical published SSPPs TLs are studied,

and compared with the microstrip line and CPW. Section V gives the fabricated TL, the measurement topology and measured S-parameters.

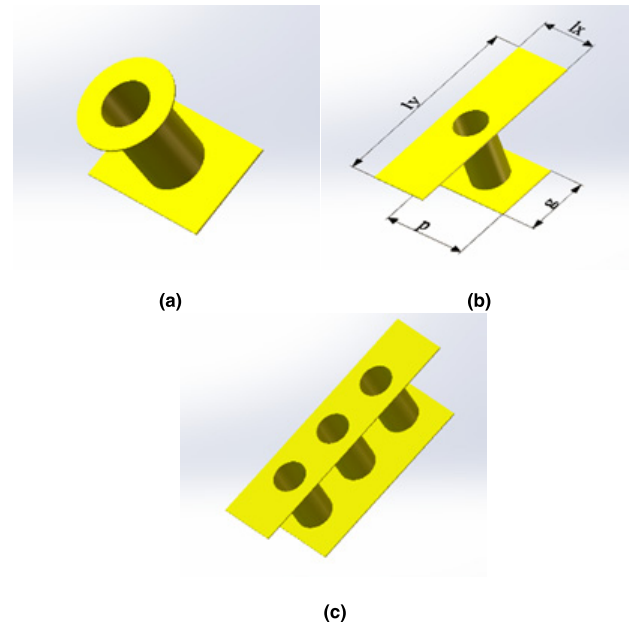


**FIGURE 1.** The schematic illustration of the unit cells. (a) The unit cell in [38]. (b) The proposed unit cell, in which  $p$  is the period,  $l_x$  and  $l_y$  are the width and length of the rectangular piece, respectively. (c) The proposed unit cell composed of several parallel metallized via holes.

## II. WORKING PRINCIPLE AND PARAMETRIC STUDY

### A. UNIT CELL STRUCTURE

The SSPPs unit cell, composed of a metal element and a metallized via hole proposed by [38], is shown in Fig. 1(a), which is planted on a ground plane. Different dispersion characteristics can be obtained by changing the radius of the element when the radius of the metallized via hole is constant. However, only one variable can be used to tailor the element, which limits its specific application. The proposed unit cell consists of a rectangular metal piece and a metallized via hole, as shown in Fig. 1(b), the dispersion characteristics can be tailored by two variables: length and width. The unit cell can be adapted to a variety of microwave integrated circuits by planting in a metal strip or a ground plane to form fully-open structures or semi-open structures. On the basis of Fig. 1(b), unit cell composed of several parallel metallized via holes is proposed, as shown in Fig. 1(c). The unit cell obtains more degrees of freedom to tailor dispersion characteristics than Fig. 1(b) by increasing the number of metallized via holes, further extending its range of applications.

### B. DISPERSION CHARACTERISTICS OF THE FUNDAMENTAL MODE

Dispersion characteristics of the proposed unit cell (Fig. 1(b)) can be obtained by eigenmode analysis of full wave simulation, as shown in Fig. 2(a). The external area is bounded by periodic boundary in the transmission direction of electromagnetic wave ( $x$ -direction), and perfect magnetic conductor

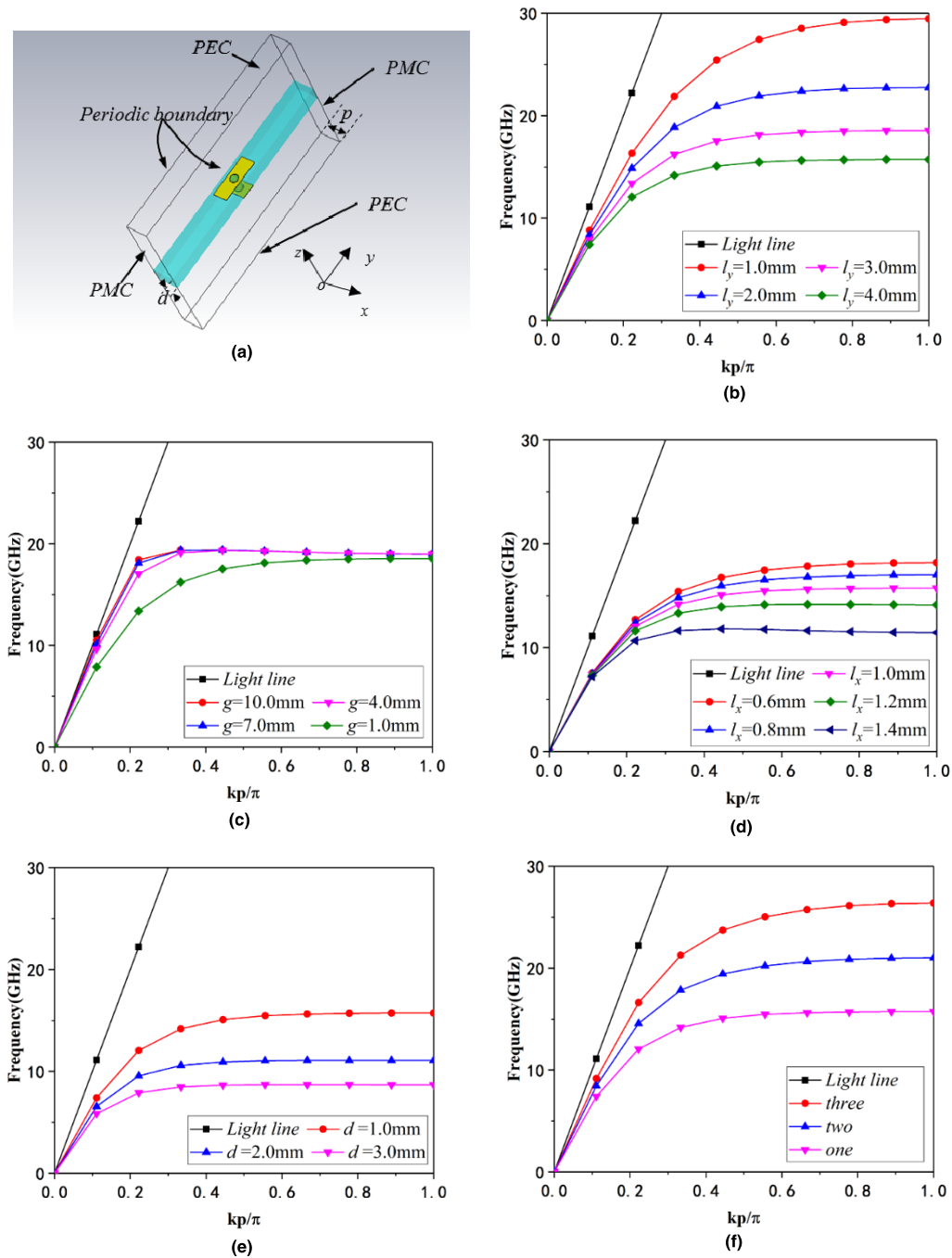


**FIGURE 2.** Relationships between the key parameters of proposed unit cell and the dispersion characteristics. The black line indicates the light line in free space. (a) Boundary settings of the eigenmode analysis,  $p$  is the period of the unit cell,  $d$  is the thickness of the F4B substrate. (b) Variation of the dispersion relationships with different values of  $l_y$ , in which  $l_x$  is 1 mm,  $d$  is 1 mm and  $g$  is 1.5 mm. (c) Variation of the dispersion relationships with different values of  $g$ , in which  $l_x$  is 1 mm,  $l_y$  is 4 mm and  $d$  is 1 mm. (d) Variation of the dispersion relationships with different values of  $l_x$ , in which  $l_y$  is 4 mm,  $d$  is 1 mm and  $g$  is 1.5 mm. (e) Variation of the dispersion relationships with different values of  $d$ , in which  $l_y$  is 4 mm,  $l_x$  is 1 mm and  $g$  is 1.5 mm. (f) Variation of the dispersion relationships with different numbers of metallized via holes, in which  $l_x$  is 1 mm and  $l_y$  is 4 mm.

boundary (PMC) in the  $y$ -direction, with perfect electric conductor (PEC) in the  $z$ -direction. The relationships between the key parameters of proposed unit cell and the dispersion characteristics are given in Fig. 2 (b), (c), (d), (e) and (f). It is shown that the dispersion relationships deviate significantly

from the light, both of which are non-radiative modes, indicating that the proposed unit cell supports the propagation of confined modes. The dispersion characteristics are determined by the structural parameters, which are similar with the typical SSPPs structures [4], [12], [40], [41].

With the increase of wave number, the dispersion relationships of the unit cells deviate from the light and eventually approach the cutoff frequency. The diameter of the metallized via hole is 0.6mm and the period  $p$  is 1.5mm.  $l_x$  is the width of the rectangular piece,  $l_y$  is the length of the rectangular piece,  $d$  is the thickness of F4B substrate and  $g$  is the width of the metal strip. Fig. 2 shows the relationship between the key parameters of the unit cell and the dispersion characteristics. When  $l_x$  is 1 mm,  $d$  is 1mm and  $g$  is 1.5mm, varying the length  $l_y$ , the dispersion relationships are obtained as shown in Fig. 2(b). The cutoff frequency of the unit cell is significantly reduced while the length of the rectangular piece is increased. When  $l_x$  is 1 mm,  $l_y$  is 3 mm and  $d$  is 1mm, varying the width  $g$ , the dispersion relationships are obtained as shown in Fig. 2(c). The cutoff frequencies are not significantly different while the width of the metal strip is varied, which indicates that the dispersion characteristics of the proposed unit cell are relatively stable. When  $l_y$  is 4 mm,  $d$  is 1mm and  $g$  is 1.5mm, varying the width  $l_x$ , the dispersion relationships are obtained as shown in Fig. 2(d). The cutoff frequency of the unit cell is significantly reduced, when the width of the rectangular piece is increased. When  $l_x$  is 1 mm,  $l_y$  is 3 mm and  $g$  is 1.5mm, varying the thickness  $d$ , the dispersion relationships are obtained as shown in Fig. 2(e). The cutoff frequency of the unit cell is significantly increased, when the thickness of the substrate is declined. Combining Fig. 2 (b), (c), (d), and (e), it can be found that the length and width of the rectangular piece of the unit cell and the thickness of substrate are very obvious for the regulation of the dispersion characteristics. And the combination of these parameters can effectively regulate the characteristics of the proposed TL. When  $l_x$  is 1 mm and  $l_y$  is 4 mm, the number of metallized via holes is increased, the dispersion characteristics are obtained as shown in Fig. 2(f). The cutoff frequency of the unit cell significantly increased, while the number of metallized via holes are increased, which indicates that the unit cell can be easily extended to a new unit cell with different dispersion characteristics.

### C. ELECTROMAGNETIC FIELD DISTRIBUTIONS OF THE FUNDAMENTAL MODE

When the frequency of the propagation wave is lower than the cutoff frequency, it can propagate along the proposed TL. The electromagnetic energy mainly exists above the surface of the unit cells. The electric-force lines are emitted from the surface of the metal pieces and terminate in the adjacent unit cells, which indicate that the electromagnetic energy is tightly trapped in the TL, as shown in Fig. 3(a). The electric field distributions and the dispersion relationship indicate this TL satisfies SSPPs transmission. The  $|E_x|$  magnitudes of the electrical field at cross section of the proposed unit cell are given in Fig. 3(b). The electric field distributions of the unit cells composed of parallel metallized via holes (Fig. 1(c)) are similar to the unit cells (Fig. 1(a) and Fig. 1(b)), as shown in Fig. 3(b).

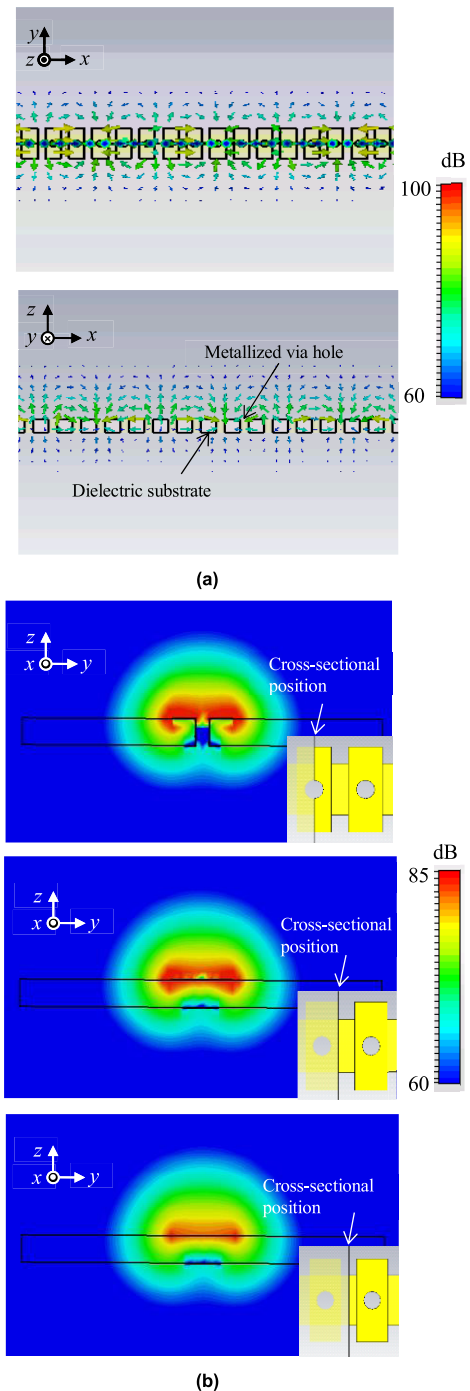


**FIGURE 3.** (a) Electric field distributions of unit cells with single metallized via hole on  $xoy$  plane and  $xoz$  plane at 19GHz, in which  $l_x$  is 1 mm,  $l_y$  is 4mm,  $d$  is 1mm,  $g$  is 1.5mm and the diameter of the metallized via hole is 0.6mm. (b)  $|E_x|$  magnitudes of electric field at central, edge of the unit cell and between two unit cells at 19GHz.

### D. CHARACTERISTICS OF HIGH-ORDER MODES

According to [26], the height of the proposed TL is limited by the thickness of the dielectric substrate so that the high-order modes in  $z$ -direction are not easily supported below millimeter frequency. Therefore, the high-order modes in the  $y$ -direction are our interest.

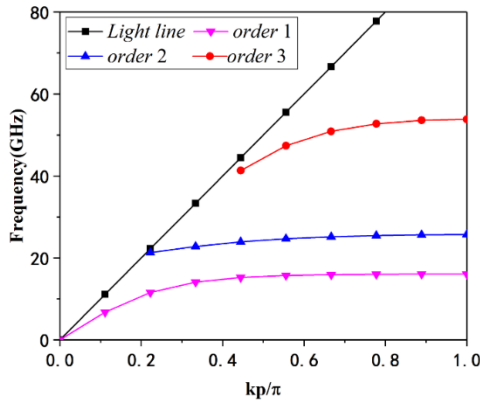


**FIGURE 4.** The dispersion relationships of the modes, in which  $l_y = 4\text{mm}$ ,  $p = 1.5\text{mm}$ ,  $l_x = 1\text{mm}$ ,  $d$  is  $1\text{mm}$  and  $g = 1.5\text{mm}$ . The black line indicates the light line in free space.

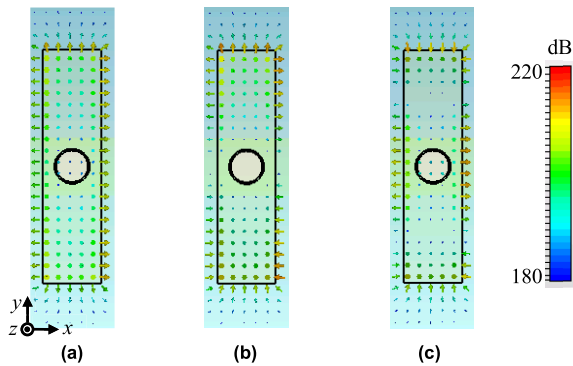


**FIGURE 5.** The electric field distributions of the modes on the proposed unit cell. (a) 1-order mode. (b) 2-order mode. (c) 3-order mode.

The purpose of this section is to investigate the performance of the modes, so we set the proposed unit cell  $l_y$  to  $4\text{mm}$  and  $p$  to  $1.5\text{mm}$ , which can support the high-order modes. The dispersion relationships and electric field distributions of different modes are given by simulations in Fig. 4 and Fig. 5, respectively. The high-order modes begin to be supported by the unit cells at the intersection point of the dispersion curves of high-order modes and light dispersion curve. Three modes are supported by the proposed unit cell at  $0\text{--}60\text{GHz}$ , whose velocities are less than the velocity of light in free space, indicating their wave numbers are greater than the wave number of the light in free space. The electric field distributions of the three modes are significantly different, which indicates that the electromagnetic field in  $y$  direction satisfies the standing wave distribution.

### III. TRANSMISSION AND CONVERSION STRUCTURE

In order to verify the performance of the proposed TL, a simple high-efficiency 2D conversion structure is utilized to convert the guided waves to the proposed 3D SSPPs TL. The proposed SSPPs TL and conversion structure are printed on  $1\text{mm}$  thick F4B substrate with dielectric constant of  $2.65$  and loss tangent of  $0.001$ . The thickness of ultrathin copper strips is selected to be  $0.018\text{mm}$ , as shown in Fig. 6. The proposed

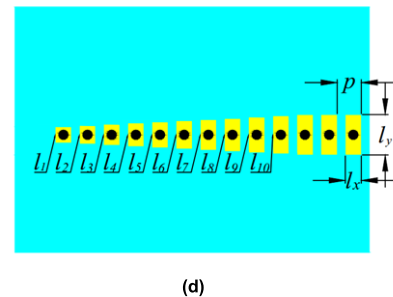
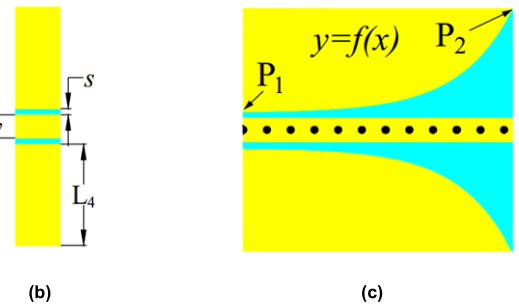
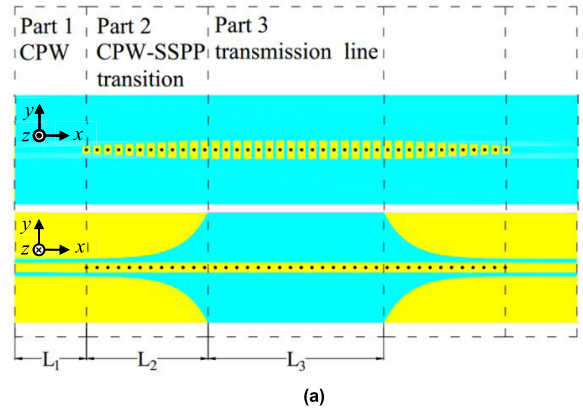


**FIGURE 6.** Structure of the proposed TL. (a) Top and bottom view of the proposed TL, in which  $L_1 = 10\text{mm}$ ,  $L_2 = 17\text{mm}$ ,  $L_3 = 24.5\text{mm}$ . (b) Part 1: CPW structure, in which  $w = 1.5\text{mm}$ ,  $s = 0.1\text{mm}$ . (c) Part 2: Bottom view of the conversion structure. (d) Part 2: Top view of the conversion structure, in which  $l_1 = 1\text{mm}$ ,  $l_{10} = 2.35\text{mm}$ .

TL is an axisymmetric structure and consists of three parts. CPW with  $50\Omega$  characteristic impedance, regard as the excitation waveguide, is denoted as Part 1, as shown in Fig. 6(a). Part 2 is the 2D conversion structure, as shown in Fig. 6(c). In order to obtain impedance matching with the proposed TL, the conversion process is accompanied by a gradual structure in which the length of the rectangular piece is from  $l_1$  to  $l_{10}$  with a step of  $0.15\text{mm}$ , as shown in Fig. 6(d). The TM wave impedance of the proposed TL is expressed by

$$Z^{TM} = -\frac{j\eta_0}{2} \sqrt{\frac{\beta^2}{k_0^2} - 1} \quad (1)$$

where  $\eta_0$  is the characteristics impedance of the free space,  $\beta$  is the wave vector in the propagation direction,  $k_0$  is the wave number in free space [42]–[44]. The impedance can be used to check the impedance matching between CPW and the proposed TL.

The Vivaldi curve of  $y = f(x)$  is expressed as

$$y = C_1 e^{\alpha x} + C_2 (x_1 < x < x_2) \quad (2)$$

where

$$C_1 = \frac{y_2 - y_1}{e^{\alpha x_2} - e^{\alpha x_1}}, \quad C_2 = \frac{y_1 e^{\alpha x_2} - y_2 e^{\alpha x_1}}{e^{\alpha x_2} - e^{\alpha x_1}}, \quad \alpha = 0.04.$$

$P_1(x_1, y_1)$  and  $P_2(x_2, y_2)$  are the start point and end point of the Vivaldi curve respectively. Part 3 is the SSPPs TL, the period  $p$  is 1.5mm, the width of the rectangular piece  $l_x$  is 1 mm and the length  $l_y$  is 2.5mm.

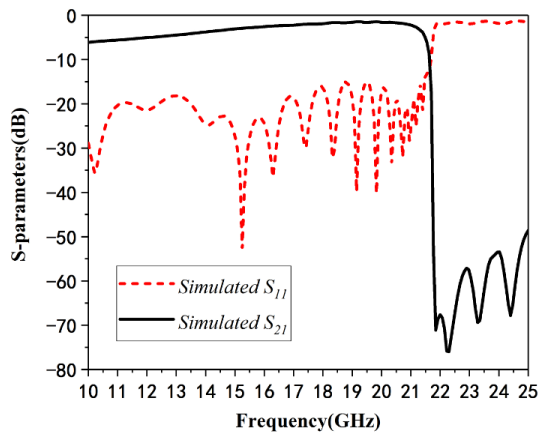


**FIGURE 7.** Simulated S-parameters of the proposed TL by using the TL model and the full wave simulation.

The S-parameters of the proposed TL are simulated by using the TL model and the full wave simulation, as shown in Fig. 7. The cutoff frequency is in accordance with the analysis of dispersion characteristics. The SSPPs waves cannot propagate above the cutoff frequency. The S-parameters indicate that electromagnetic waves can propagate efficiently along the TL.

#### IV. TRANSMISSION LOSSES

The transmission loss of the SSPPs TL is a very important indicator, especially at high frequencies. The total losses of the SSPPs TL (Fig. 1(a) and Fig. 8(d)) are studied by [38] and [45], which includes ohmic loss, dielectric loss and radiation loss. For different TLs, the ohmic loss, dielectric loss and radiation loss have different occupation rates in total losses due to their different transmission modes. Therefore, the total losses can not reflect the actual loss characteristics of the TLs. The ohmic loss of the double sides comb-like SSPPs TL was investigated and compared with CPW. However, the dielectric loss was not studied [43]. Accordingly, in this section, the ohmic losses and dielectric losses of the proposed TL and some typical published SSPPs TLs are studied and compared with the microstrip line and CPW by simulations.

To assess the dielectric losses, the proposed TL and the published SSPPs TLs with its copper metal replaced by PEC are simulated. On the other hand, the proposed TL and the published SSPPs TLs on lossless substrates are simulated to

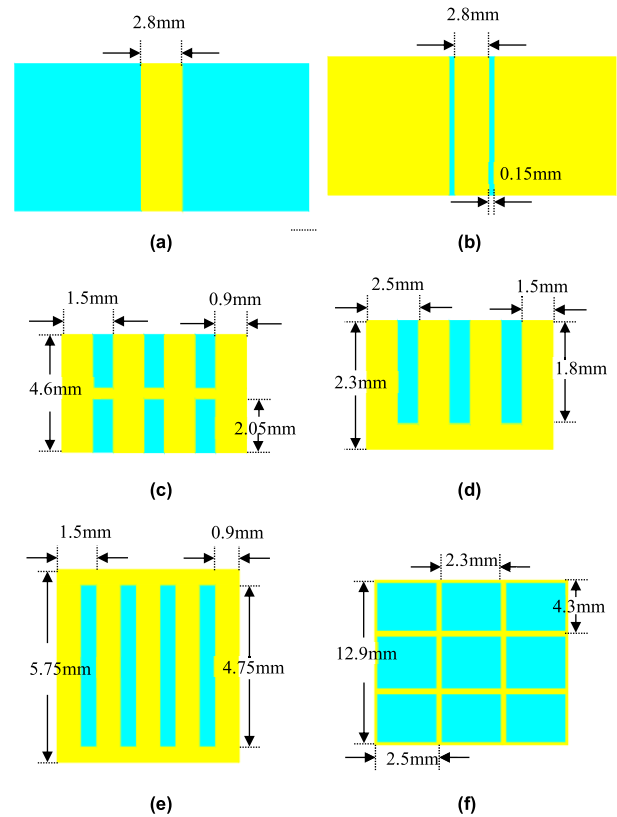


**FIGURE 8.** The array structures and detailed parameters of the published TLs. (a) 50Ω microstrip line. (b) 50Ω coplanar waveguide. (c) Double sides comb-like TL. (d) Single side comb-like TL. (e) SSPPs TL proposed by [47]. (f) SSPPs TL proposed by [44].

evaluate the ohmic losses. In order to eliminate the effects of conversion loss conveniently, the Bianco-Parodi (BP) method is adopted [46]. This method cannot be used to analyze the radiation loss, because the radiation loss varies nonlinearly with the length of the SSPPs TLs. The method of obtaining the radiation loss of double sides comb-like SSPPs TL (Fig. 8(c)) is complex and not very accurate [39]. Therefore, the radiation loss is not discussed in this paper.

The ohmic losses and dielectric losses of the proposed TL, double sides comb-like TL, single side comb-like TL, SSPPs TL proposed by [44] and SSPPs TL proposed by [47] are compared with the 50Ω microstrip line and 50Ω CPW. The array structures and detailed parameters of the TLs are given in Fig.8. The dielectric substrate of these TLs are 1mm thick F4B substrate with dielectric constant of 2.65 and loss tangent of 0.001. The cutoff frequencies of these published SSPPs TLs are similar to the proposed TL ( $l_x$  is 1 mm,  $l_y$  is 4mm and the diameter of the metallized via hole is 0.6mm). The dispersion characteristics of the proposed TL and these published SSPPs TLs are given in Fig.9. The ohmic losses and the dielectric losses are given in Fig. 10 and Fig. 11, respectively.

From the comparison of ohmic losses and dielectric losses, we can find that the ohmic losses and dielectric losses of the proposed TL are comparable to single side comb-like TL, SSPPs TL proposed by [44] and SSPPs TL proposed by [47].

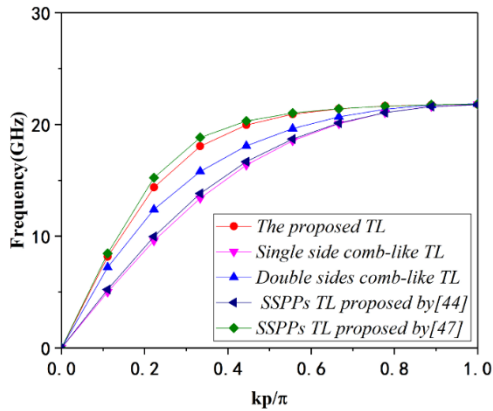


FIGURE 9. The dispersion characteristics of the published SSPPs TLs and the proposed TL.

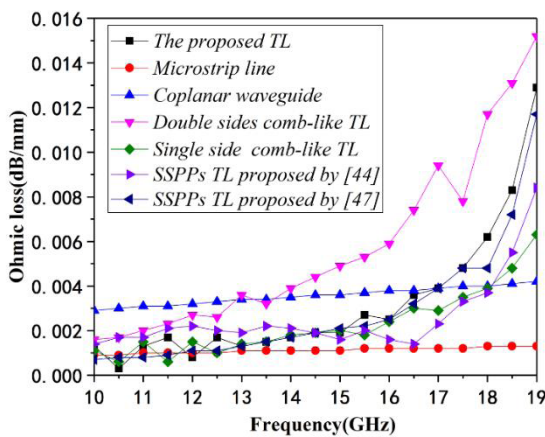


FIGURE 10. Simulated ohmic losses of the proposed TL, 50Ω microstrip line, 50Ω coplanar waveguide, double sides comb-like TL, single side comb-like TL, SSPPs TL proposed by [44], SSPPs TL proposed by [47].

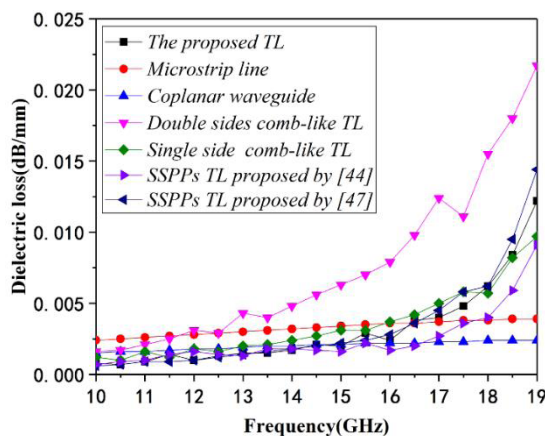


FIGURE 11. Simulated dielectric losses of the proposed TL, 50Ω microstrip line, 50Ω coplanar waveguide, double sides comb-like TL, single side comb-like TL, SSPPs TL proposed by [44], SSPPs TL proposed by [47].

The ohmic loss and dielectric loss of the double sides comb-like TL are higher than other SSPPs TLs. The ohmic losses of these SSPPs TLs are less than the CPW at low frequencies and higher than the microstrip line, while the dielectric losses are lower than the microstrip line and CPW. This phenomenon is

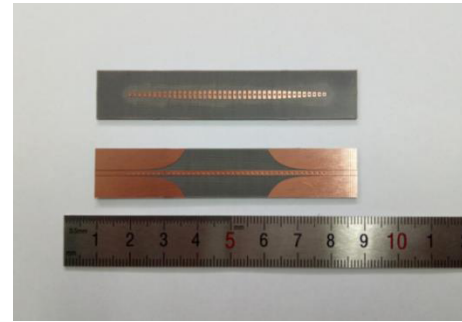


FIGURE 12. The photograph of the fabricated TL.

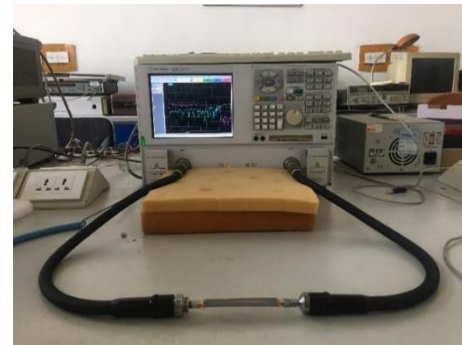


FIGURE 13. The photograph of the measurement topology.

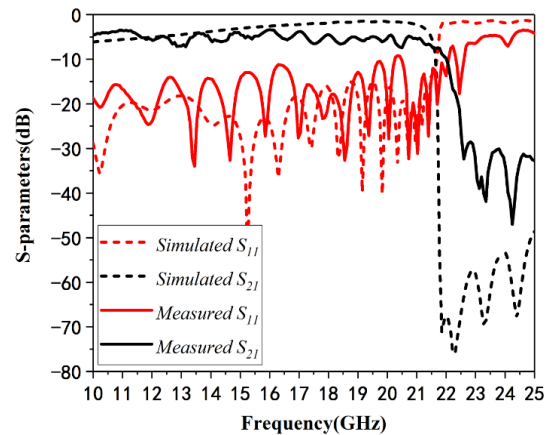


FIGURE 14. Simulated and measured S-parameters of the proposed TL.

caused by the fact that the electromagnetic energy of SSPPs TL is mainly concentrated on the metal surface and upper half-space of the unit cell.

## V. FABRICATION AND MEASUREMENT

The proposed TL is fabricated according to the parameters of Fig. 6, as shown in Fig. 12. It is measured by an Agilent Technologies E8363B network analyzer, as shown in Fig. 13. The simulated and measured S-parameters are given in Fig. 14. The S-parameters of measured are close to the simulation from 10 to 21GHz, indicating that the proposed TL has relatively good transmission performance in this frequency range. Differences between the simulated and measured are mainly caused by the mismatch between SMA connectors and the

conversion structure of the proposed TL, and the fabrication tolerances.

## VI. CONCLUSION

In this paper, a novel 3D integrated SSPPs TL is proposed. The dispersion characteristics and electric field distributions of fundamental mode and high-order modes are analyzed and simulated. Different dispersion characteristics can be obtained by tailoring the parameters of the unit cells. The proposed TL structures have an army of adjustable parameters, which can be easily tailored according to different application scenarios. The ohmic losses and dielectric losses of the proposed TL and some typical published SSPPs TLs are investigated and compared with the microstrip line and CPW. The comparison of the ohmic losses and dielectric losses between SSPPs TLs and conventional TLs indicates the low loss characteristics and potential for specific applications of the SSPPs TLs. The proposed TL is simulated and experimented, which verifies the conversion structure between CPW and the proposed TL is effective. The proposed TL has a common metal strip and two-layer-metal structure as the bases, making it more convenient to integrate with existing microwave circuits and systems and laying the foundation for developing high-performance SSPPs systems in the future.

## REFERENCES

- [1] S. A. Maier, *Plasmonics: Fundamentals and Applications*. New York, NY, USA: Springer, 2007.
- [2] W. L. Barnes, A. Dereux, and T. W. Ebbesen, "Surface plasmon subwavelength optics," *Nature*, vol. 424, no. 6950, pp. 824–830, Aug. 2003.
- [3] M. Sandtke and L. Kuipers, "Slow guided surface plasmons at telecom frequencies," *Nature Photon.*, vol. 1, no. 10, pp. 573–576, Sep. 2007.
- [4] R. Elliott, "On the theory of corrugated plane surfaces," *Trans. IRE Prof. Group Antennas Propag.*, vol. 2, no. 2, pp. 71–81, Apr. 1954.
- [5] N. Fang, H. Lee, C. Sun, and X. Zhang, "Sub-diffraction-limited optical imaging with a silver superlens," *Science*, vol. 308, no. 5721, pp. 534–537, Apr. 2005.
- [6] Z. W. Liu, Q. H. Wei, and X. Zhang, "Surface plasmon interference nanolithography," *Nano Lett.*, vol. 5, no. 5, pp. 957–961, Apr. 2005.
- [7] A. P. Hibbins, B. R. Evans, and J. R. Sambles, "Experimental verification of designer surface plasmons," *Science*, vol. 308, no. 5722, pp. 670–672, Apr. 2005.
- [8] J. G. Rivas, C. Schotsch, P. H. Bolivar, and H. Kurz, "Enhanced transmission of THz radiation through subwavelength holes," *Phys. Rev. B*, vol. 68, no. 20, Oct. 2003, Art. no. 201306.
- [9] H. Cao and A. Nahata, "Resonantly enhanced transmission of terahertz radiation through a periodic array of subwavelength apertures," *Opt. Express*, vol. 12, no. 6, pp. 1004–1010, Apr. 2004.
- [10] H. Cao and A. Nahata, "Influence of aperture shape on the transmission properties of a periodic array of subwavelength apertures," *Opt. Express*, vol. 12, no. 16, pp. 3664–3672, 2004.
- [11] J. B. Pendry, L. Martín-Moreno, and F. J. Garcia-Vidal, "Mimicking surface plasmons with structured surfaces," *Science*, vol. 305, pp. 847–848, Aug. 2004.
- [12] F. J. Garcia-Vidal, L. Martín-Moreno, and J. B. Pendry, "Surfaces with holes in them: New plasmonic metamaterials," *J. Opt. A, Pure Appl. Opt.*, vol. 7, no. 2, pp. 97–101 Jan. 2005
- [13] Y. J. Zhou, Q. Jiang, and T. J. Cui, "Three-dimensional subwavelength components utilizing THz surface plasmons," *Sci. China Inf. Sci.*, vol. 55, no. 1, pp. 79–89, Jan. 2012.
- [14] M. Aghadjani and P. Mazumder, "Terahertz switch based on waveguide-cavity-waveguide comprising cylindrical spoof surface plasmon polariton," *IEEE Trans. Electron Devices*, vol. 62, no. 4, pp. 1312–1318, Apr. 2015.
- [15] M. Aghadjani and P. Mazumder, "THz polarizer controller based on cylindrical spoof surface plasmon polariton (C-SSPP)," *IEEE Trans. Terahertz Sci. Technol.*, vol. 5, no. 4, pp. 556–563, Jul. 2015.
- [16] J. T. Shen, P. B. Catrysse, and S. Fan, "Mechanism for designing metallic metamaterials with a high index of refraction," *Phys. Rev. Lett.*, vol. 94, no. 19, 2005, Art. no. 197401.
- [17] X. F. Zhang, L. Shen, and L. Ran, "Low-frequency surface plasmon polaritons propagating along a metal film with periodic cut-through slits in symmetric or asymmetric environments," *Appl. Phys.*, vol. 105, no. 1. Feb. 2005, Art. no. 013704.
- [18] M. L. Nesterov *et al.*, "Geometrically induced modification of surface plasmons in the optical and telecom regimes," *Opt. Lett.*, vol. 35, no. 3, pp. 423–425, Feb. 2010.
- [19] T. Jiang *et al.*, "Realization of tightly confined channel plasmon polaritons at low frequencies," *Appl. Phys. Lett.*, vol. 99, no. 26, p. 1119, Dec. 2011.
- [20] J. J. Wu, C. J. Wu, D. J. Hou, K. Liu, and T. J. Yang, "Propagation of low-frequency spoof surface plasmon polaritons in a bilateral cross-metal diaphragm channel waveguide in the absence of bandgap," *IEEE Photon. J.*, vol. 7, no. 1, pp. 1–8, Feb. 2015.
- [21] N. Koja, J. C. Young, and T. Suzuki, "Quasi-three-dimensional post-array for propagation and focusing of a terahertz spoof surface plasmon polariton," *Appl. Phys. A, Solids Surf.*, vol. 120, no. 2, pp. 479–485, Aug. 2015.
- [22] X. Shen, T. J. Cui, D. Martín-Cano, and F. J. Garcia-Vidal, "Conformal surface plasmons propagating on ultrathin and flexible films," *Proc. Nat. Acad. Sci. USA*, vol. 110, no. 1, pp. 40–45, 2012.
- [23] H. F. Ma, X. Shen, Q. Cheng, W. X. Jiang, and T. J. Cui, "Broadband and high-efficiency conversion from guided waves to spoof surface plasmon polaritons," *Laser Photon. Rev.*, vol. 8, no. 1, pp. 146–151, Nov. 2013.
- [24] Z. Liao, J. Zhao, B. C. Pan, X. P. Shen, and T. J. Cui, "Broadband transition between microstrip line and conformal surface plasmon waveguide," *J. Phys. D, Appl. Phys.*, vol. 47, no. 31, p. 315103, Jul. 2014.
- [25] A. Kianinejad, Z. N. Chen, and C.-W. Qiu, "Design and modeling of spoof surface plasmon modes-based microwave slow-wave transmission line," *IEEE Trans. Microw. Theory Techn.*, vol. 63, no. 6, pp. 1817–1825, Jun. 2015.
- [26] X. Liu, Y. Feng, B. Zhu, J. Zhao, and T. Jiang, "High-order modes of spoof surface plasmonic wave transmission on thin metal film structure," *Opt. Express*, vol. 8, pp. 91–102, Jan. 2009.
- [27] H. Yao, S. Zhong, and W. Tu, "Performance analysis of higher mode spoof surface plasmon polariton for terahertz sensing," *J. Appl. Phys.*, vol. 117, no. 13, Apr. 2015, Art. no. 133104.
- [28] K. D. Xu, Y. J. Guo, and X. Deng, "Terahertz broadband spoof surface plasmon polaritons using high-order mode developed from ultra-compact split-ring grooves," *Opt. Express*, vol. 27, no. 4, pp. 4354–4363, Feb. 2019.
- [29] Y. J. Zhou and B. J. Yang, "Planar spoof plasmonic ultra-wideband filter based on low-loss and compact terahertz waveguide corrugated with dumbbell grooves," *Appl. Opt.*, vol. 54, no. 14, pp. 4529–4533, May 2015.
- [30] X. Gao *et al.*, "Ultrathin dual-band surface plasmonic polariton waveguide and frequency splitter in microwave frequencies," *Appl. Phys. Lett.*, vol. 102, no. 15, Apr. 2013, Art. no. 151912.
- [31] M. Z. Hu *et al.*, "Ultra-wideband filtering of spoof surface plasmon polaritons using deep subwavelength planar structures," *Sci. Rep.*, vol. 6, Nov. 2016, Art. no. 37065.
- [32] H. C. Zhang, S. Liu, X. Shen, L. H. Chen, L. Li, and T. J. Cui, "Broadband amplification of spoof surface plasmon polaritons at microwave frequencies," *Laser Photon. Rev.*, vol. 9, no. 1, pp. 83–90, Jan. 2014.
- [33] H. C. Zhang *et al.*, "Second-harmonic generation of spoof surface plasmon polaritons using nonlinear plasmonic metamaterials," *ACS Photon.*, vol. 3, no. 1, pp. 139–146, May 2015.
- [34] G. S. Kong, H. F. Ma, B. G. Cai, and T. J. Cui, "Continuous leaky-wave scanning using periodically modulated spoof plasmonic waveguide," *Sci. Rep.*, vol. 6, Jul. 2016, Art. no. 29600.
- [35] S. Zhao, H. C. Zhang, J. Zhao, and W. X. Tang, "An ultra-compact rejection filter based on spoof surface plasmon polaritons," *Sci. Rep.*, vol. 7, Sep. 2017, Art. no. 10576.
- [36] Y. J. Guo, K. D. Xu, Y. Liu, and X. Tang, "Novel surface plasmon polariton waveguides with enhanced field confinement for microwave-frequency ultra-wideband bandpass filters," *IEEE Access*, vol. 6, pp. 10249–10256, 2018.
- [37] Y. J. Guo, K. D. Xu, and X. Tang, "Spoof plasmonic waveguide developed from coplanar stripline for strongly confined terahertz propagation and its application in microwave filters," *Opt. Express*, vol. 26, no. 8, pp. 10589–10598, Apr. 2018.



- [38] J. F. Zhu, S. W. Lion, S. Fang, and Q. Xue, "Half-spaced substrate integrated spoof surface plasmon polaritons based transmission line," *Sci. Rep.*, vol. 7, Aug. 2017, Art. no. 8013.
- [39] Z. Xu, S. Li, X. Yin, H. Zhao, and L. Liu, "Radiation loss of planar surface plasmon polaritons transmission lines at microwave frequencies," *Sci. Rep.*, vol. 7, Jul. 2017, Art. no. 6098.
- [40] S. A. Maier et al., "Terahertz Surface plasmon-polariton propagation and focusing on periodically corrugated metal wires," *Phys. Rev. Lett.*, vol. 97, no. 17, Oct. 2017, Art. no. 176805.
- [41] Q. Gan, Z. Fu, Y. J. Ding, and F. J. Bartoli, "Ultrawide-bandwidth slow-light system based on THz plasmonic graded metallic grating structures," *Phys. Rev. Lett.*, vol. 101, no. 25, Jun. 2008, Art. no. 256803.
- [42] R. F. Harrington, *Time-Harmonic Electromagnetic Fields*. New York, NY, USA: McGraw-Hill, 1961.
- [43] A. Kianinejad, Z. N. Chen, and C.-W. Qiu, "Low-loss spoof surface plasmon slow-wave transmission lines with compact transition and high isolation," *IEEE Trans. Microw. Theory Techn.*, vol. 64, no. 10, pp. 3078–3086, Oct. 2016.
- [44] S. Ge et al., "Single-side-scanning surface waveguide leaky-wave antenna using spoof surface plasmon excitation," *IEEE Access*, vol. 6, pp. 66020–66029, 2018.
- [45] H. C. Zhang, Q. Zhang, J. F. Liu, W. Tang, Y. Fan, and T. J. Cui, "Smaller-loss planar SPP transmission line than conventional microstrip in microwave frequencies," *Sci. Rep.*, vol. 6, Mar. 2016, Art. no. 23396.
- [46] B. Bianco and M. Parodi, "Determination of the propagation constant of uniform microstrip lines," *Amer. J. Kidney Diseases*, vol. 45, no. 45, pp. 107–110, Jan. 1976.
- [47] L. Liu et al., "Multi-channel composite spoof surface plasmon polaritons propagating along periodically corrugated metallic thin films," *J. Appl. Phys.*, vol. 116, no. 1, Jul. 2014.



**SENSONG SHEN** is currently pursuing the Ph.D. degree with the School of Physics, University of Electronic Science and Technology of China. His research interests include microwave wave circuits and systems, and spoof surface plasmon polaritons theory and application.



**BING XUE** received the M.S. degree in the microwave engineering from the Institute of Electronics, Chinese Academy of Sciences, in 2017. He is currently pursuing the Ph.D. degree with the University of Electronic Science and Technology of China. He has authored or co-authored ten papers in his research fields. His research interests include computational electromagnetics, microwave filters and low-frequency electromagnetic wave propagation on the earth and antennas.



**MENGXIA YU** received the master's and Ph.D. degrees in engineering from the University of Electronic Science and Technology of China, in 1997 and 2005, respectively. She is currently a Researcher with the School of Physics, University of Electronic Science and Technology of China, Chengdu, China. She has authored or co-authored more than 20 papers and eight patents in her research fields. Her research interests include microwave wave circuits and systems, circuit devices, system in package circuits, bioelectromagnetic effects, and Terahertz circuits and systems.



**JUN XU** received the bachelor's degree of engineering from the Chengdu Institute of Telecommunication, in 1984, and the master's degree of engineering from the University of Electronic Science and Technology of China, in 1990. He was promoted to a Professor in 2000. He has long been engaged in basic research, applied basic research, and teaching of electromagnetic field and microwave technique, and radio physics. He published more than 80 academic papers, and more than 30 of them were included by SCI and EI. His research interests include microwave and millimeter wave theory and techniques, millimeter wave hybrid integration techniques, microwave and millimeter wave devices/circuits and systems, millimeter wave communication technique, key techniques, and systems of millimeter wave radar. In 2005, his three dimensional microwave integrated circuits electromagnetic modeling method and new device research project won the second prize of Natural Scientific Award of National Scientific and Technological Award of the Ministry of Education of China.

...